

Fluid Flow Equations for Rotordynamic Flows in Seals and Leakage Paths

Y. Hsu

C. E. Brennen

Professor

Division of Engineering and Applied Science,
California Institute of Technology,
Pasadena, CA 91125

Fluid-induced rotordynamic forces produced by the fluid in an annular seal or in the leakage passage surrounding the shroud of a pump or turbine, are known to contribute substantially to the potential excitation forces acting on the rotor. The present research explores some of the important features of the equations governing bulk-flow models of these flows. This in turn suggests methods which might be used to solve these bulk-flow equations in circumstances where the linearized solutions may not be accurate. This paper presents a numerical method for these equations and discusses comparison of the computed results with experimental measurements for annular seals and pump leakage paths. [DOI: 10.1115/1.1436093]

Introduction

Over the last few years a substantial body of experimental data has been gathered on fluid-induced rotordynamic forces [1] generated in narrow, fluidfilled annuli such as occur in turbulent annular seals (for example, Childs and Dressman [2], Nordmann and Massmann [3]) or in the leakage flows surrounding the shrouded impellers of pumps or turbines (for example, Guinzburg et al. [4]). To allow for greater understanding of the underlying fluid mechanics of such flows, it is clearly valuable to view this data in the context of an accurate analytical model and, if necessary, to tune the frictional and other parameters in the model to provide a reliable tool for the designer.

The problem with this strategy is that the available analytical models have not yet shown themselves capable of accurate and reliable predictions. Perhaps the most promising approach has been the bulk flow model developed by Childs [5,6] and subsequently used by others [7]. This linearized model appears to give reasonable results in some cases and unreasonable, even bizarre results, in others. Nevertheless, it represents a coherent and rational starting point from which to begin. Some of the inherent problems with this model are summarized in the following section.

Bulkflow Models of Rotordynamic Flows

Based on Hirs [8] lubrication equations, the bulk flow model of Childs [6] uses simple correlations for the shear stresses based on the gap averaged flow velocities. This model, in its perturbation solution form, is widely regarded as a useful rotordynamic analysis tool for problems with relatively simple computational domains. As presented by Childs, the bulk flow model assumes that the three-dimensional, unsteady, turbulent flow in an annulus can be accurately approximated by reducing the dimensions of the flow from three to two, by using a simple correlation between the shear stresses and gap averaged velocities, and by treating the rotordynamic flow as a linear perturbation on the mean flow. Each of these assumptions should be carefully considered when using this approach to model the flow in a more complex computational domain such as a centrifugal pump leakage annulus.

The assumption that the dimensions of the flow can be reduced from three to two implies that the velocity profiles within the annulus are self-similar and therefore, that the equations of the flow can be averaged over the gap without excessive error. This may have limitations under certain conditions noted in experi-

ments in which flow reversals and recirculation zones occur in the leakage path (Sivo et al. [9], Guelich et al. [10]). These changes in flow direction may lead to frictional stresses which are acting in a direction different from that predicted by the gap averaged velocity. Certain 3-D computational analyses, such as Baskharone and Hensel [11], have observed these flow reversals.

The Reynolds number of most leakage flows is very high. This means the bulk flow model requires expressions which relate the turbulent shear stresses to the averaged velocities in the gap. In the current form of the bulk flow model, the shear stresses on the rotor and the stator are calculated using friction coefficients [8]. These are defined by:

$$\frac{\tau}{\frac{1}{2}\rho u^2} = n \left(\frac{\rho u h}{\eta} \right)^m \quad (1)$$

where u is the gap-averaged velocity relative to the surface under consideration, and the m and n are denoted by m_S and n_S for the stator and m_R and n_R for the rotor. These expressions, which are a simple and heuristic extrapolation from the correlations for turbulent flow in a pipe, are taken from the work of Hirs who recommends that the coefficients m and n be "fitted to individual experiments." The frictional coefficients are dependent on six physical parameters, including the curvature of the surface, inertial effects, and roughness. Thus, the coefficients may not fully account for the curvature of the flow path in a particular leakage geometry. As stated previously any reversal in flow direction near the impeller implies a serious error in the correlation of Eq. (1). The sign of the wall-shear stress term for the rotor should change in a region of reverse flow.

In addition, the use of the above expressions for the turbulent shear stresses are subject to an even more general criticism. They are correlations for steady turbulent flows based, primarily, on experimental observations of steady flows. In contrast, the rotordynamic flows of concern here are fundamentally unsteady. The problem is that very little is known about turbulent flows which are unsteady in the sense that the flow is being externally excited. Therefore, correlations such as that given above are only useful because there are no alternatives, and it must be recognized that the unsteady flows of the present context may lead to substantial deviations from these correlations. At present, this issue can only be resolved by careful comparison of the experimental and model results.

Finally, Childs treats the rotordynamic flow as a linear perturbation on the mean flow in the annulus. While this may be an

Contributed by the Fluids Engineering Division for publication in the JOURNAL OF FLUIDS ENGINEERING. Manuscript received by the Fluids Engineering Division April 17, 2001; revised manuscript received October 15, 2001. Associate Editor: Y. Tsujimoto.

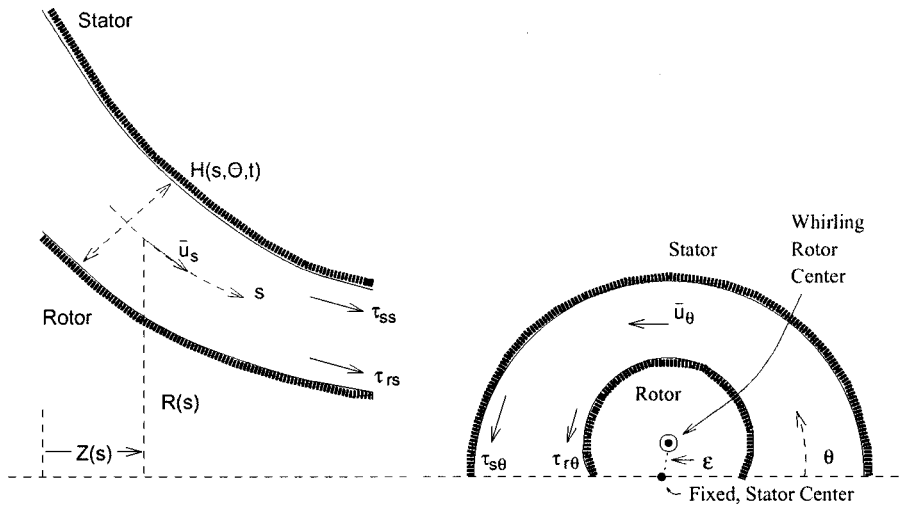


Fig. 1 Sketch of fluid filled annulus between a rotor and a stator for turbulent lubrication analysis

accurate assumption for very small eccentricities, there is currently no way to know at what eccentricity this linearization begins to lose accuracy. This paper will present a solution method that will solve the full bulk flow equations and will provide some idea as to the contribution of the nonlinear terms.

The Bulk Flow Model Equations

Black and his co-workers [12,13] were the first to attempt to identify and model the rotordynamics of turbulent annular seals. Bulk flow models (similar to those of Reynolds lubrication equations) were used. Several deficiencies in this early work caused Childs [14,15] to publish a revised version of the bulk flow model for turbulent annular seals [16] and, later, to extend this model [5,6] to examine the rotordynamic characteristics of discharge-to-suction leakage flows around shrouded centrifugal pump impellers. A general geometry is sketched in Fig. 1, and is described by coordinates of the meridian of the gap as given by $Z(s)$ and $R(s)$, $0 < s < S$, where the coordinate, s , is measured along that meridian. The clearance is denoted by $H(s, \Theta, t)$ where the mean, non-whirling clearance is given by $\bar{H}(s)$.

The equations governing the bulk flow are averaged over the gap. This leads to a continuity equation of the form

$$\frac{\partial H}{\partial t} + \frac{\partial}{\partial s}(Hu_s) + \frac{1}{R} \frac{\partial}{\partial \Theta}(Hu_\Theta) + \frac{Hu_s}{R} \frac{\partial R}{\partial s} = 0 \quad (2)$$

where u_s and u_Θ are gap-averaged velocities in the s and Θ directions. The meridional and circumferential momentum equations are

$$-\frac{1}{\rho} \frac{\partial p}{\partial s} = \frac{\tau_{Ss}}{\rho H} + \frac{\tau_{Rs}}{\rho H} - \frac{u_\Theta^2}{R} \frac{\partial R}{\partial s} + \frac{\partial u_s}{\partial t} + \frac{u_\Theta}{R} \frac{\partial u_s}{\partial \Theta} + u_s \frac{\partial u_s}{\partial s} \quad (3)$$

$$-\frac{1}{\rho R} \frac{\partial p}{\partial \Theta} = \frac{\tau_{S\Theta}}{\rho H} + \frac{\tau_{R\Theta}}{\rho H} + \frac{\partial u_\Theta}{\partial t} + \frac{u_\Theta}{R} \frac{\partial u_\Theta}{\partial \Theta} + u_s \frac{\partial u_\Theta}{\partial s} + \frac{u_\Theta u_s}{R} \frac{\partial R}{\partial s} \quad (4)$$

These are the equations used by Childs [5,6]. Note that they include not only the viscous terms commonly included in Reynolds lubrication equations (see for example Pinkus and Sternlicht [17]) but also the inertial terms (see Fritz [18]) which are necessary for the evaluation of the rotordynamic coefficients.

Using Hirs' [8] approach, the turbulent shear stresses, τ_{Ss} and $\tau_{S\Theta}$, applied to the stator by the fluid in the s and Θ directions are given by:

$$\frac{\tau_{Ss}}{\rho u_s} = \frac{\tau_{S\Theta}}{\rho u_\Theta} = \frac{n_S}{2} [u_s^2 + u_\Theta^2]^{m_S + 1/2} (H/\nu)^{m_S} \quad (5)$$

and the stresses, τ_{Rs} and $\tau_{R\Theta}$, applied to the rotor by the fluid in the same directions:

$$\frac{\tau_{Rs}}{\rho u_s} = \frac{\tau_{R\Theta}}{\rho(u_\Theta - \Omega R)} = \frac{n_R}{2} [u_s^2 + (u_\Theta - \Omega R)^2]^{m_R + 1/2} (H/\nu)^{m_R} \quad (6)$$

where the constants n_S , n_R , m_S and m_R are chosen to fit the available data on turbulent shear stresses. Childs [14] uses typical values of these constants from simple pipe flow correlations:

$$n_S = n_R = 0.079; \quad m_S = m_R = -0.25 \quad (7)$$

Childs then proceeds to linearize the equations by dividing the clearance, pressure, and velocities into mean components (subscript 0) that would pertain in the absence of whirl, and small, linear perturbations (subscript 1) due to an eccentric motion of the rotor at an eccentricity ϵ and a whirl frequency of ω . He develops differential equations for the coefficients which are functions of r only, with the perturbation velocities restrained to simple harmonic functions of Θ .

For a case with a steady whirl of frequency ω , and constant eccentricity ϵ , superimposed on the shaft rotation of radian frequency Ω , a method of solving the bulk flow equations using a stream function and vorticity will now be formulated. With this set of assumptions, the fluid flow in a frame of reference rotating at ω is steady and it is appropriate to rewrite the equations and solve them in this rotating frame. Defining, therefore, a new angular variable, θ , and a new angular velocity, u_θ , in this rotating frame such that

$$\theta = \Theta - \omega t; \quad u_\theta = u_\Theta - \omega R \quad (8)$$

it follows that the continuity equation, Eq. (2) can be written as

$$\frac{\partial}{\partial \theta} \{Hu_\theta\} + \frac{\partial}{\partial s} \{RHu_s\} = 0 \quad (9)$$

and this is most easily satisfied by defining a stream function, $\psi(s, \theta)$ such that

$$u_s = \frac{1}{RH} \frac{\partial \psi}{\partial \theta}; \quad u_\theta = -\frac{1}{H} \frac{\partial \psi}{\partial s} \quad (10)$$

It follows that the total volume flow rate, Q , at any meridional location, s , is given by

$$Q = \psi(s, 2\pi) - \psi(s, 0) \quad (11)$$

and this provides a periodic boundary condition on ψ in the θ direction.

In the rotating frame of reference, the equations of motion are usefully written using an appropriate total pressure, P , instead of the static pressure, p , where

$$\frac{P}{\rho} = \frac{p}{\rho} + \frac{1}{2}(u_s^2 + u_\theta^2 - R^2 \omega^2) \quad (12)$$

and the equations of motion, Eqs. (3) and (4), then become

$$\frac{\partial}{\partial s} \left(\frac{P}{\rho} \right) = -Hu_\theta \Gamma - u_s(g_S + g_R) \quad (13)$$

$$\frac{1}{R} \frac{\partial}{\partial \theta} \left(\frac{P}{\rho} \right) = Hu_s \Gamma - (u_\theta + \omega R)(g_S + g_R) + \Omega R g_R \quad (14)$$

where the functions, g_S and g_R , are the shear stress terms for the stator and rotor respectively. Using correlations (5) and (6)

$$g_S = \frac{n_S}{2H} \left(\frac{H}{\nu} \right)^{m_S} \{u_s^2 + (u_\theta + \omega R)^2\}^{m_S + 1/2} \quad (15)$$

$$g_R = \frac{n_R}{2H} \left(\frac{H}{\nu} \right)^{m_R} \{u_s^2 + (u_\theta + \omega R - \Omega R)^2\}^{m_R + 1/2} \quad (16)$$

The quantity, Γ , given by

$$\Gamma = \frac{1}{H} \left[-\frac{1}{R} \frac{\partial}{\partial s} (Ru_\theta + \omega R^2) + \frac{1}{R^2} \frac{\partial}{\partial \theta} (Ru_s) \right] \quad (17)$$

plays a crucial role both in understanding the fluid mechanics of these flows and in the solution methodology. This quantity, Γ , can be termed an ‘‘effective vorticity’’, and the existence of such a quantity has led to the development of the current methodology.

The vorticity, Γ , is a fundamental property of the flow; this can be discerned by eliminating P from Eqs. (13) and (14) to obtain the basic convection equation for Γ :

$$u_s \frac{\partial \Gamma}{\partial s} + u_\theta \frac{1}{R} \frac{\partial \Gamma}{\partial \theta} = \frac{1}{RH} \left[\frac{\partial}{\partial s} \{R(u_\theta + \omega R)(g_S + g_R) - \Omega R^2 g_R\} - \frac{\partial}{\partial \theta} \{u_s(g_S + g_R)\} \right] \quad (18)$$

which demonstrates that, in the absence of viscous effects ($g_S = g_R = 0$), the vorticity is invariant along any streamline. Conversely, the shear stresses are alone responsible for any change in Γ along a streamline. The total pressure is obtained by integration similar to that for the vorticity, Γ . From Eqs. (13) and (14) it follows that

$$u_s \frac{\partial P}{\partial s} + u_\theta \frac{1}{R} \frac{\partial P}{\partial \theta} = \frac{1}{(u_s^2 + u_\theta^2)^{1/2}} \times [\Omega R u_\theta g_R - \{u_s^2 + u_\theta(u_\theta + \omega R)\}(g_R + g_S)] \quad (19)$$

which demonstrates that the total pressure (or energy in the flow) is constant along a streamline in the absence of viscous effects. Furthermore, when written in the above manner, the governing equations, (18) and (19), indicate a physically reasonable approach to their numerical solution by iterative means.

Boundary Conditions and Numerical Methods

It follows from the above that one method for the numerical solution of the equations for a rotordynamic flow would be to proceed as follows:

(1) First, for given or guessed values of the vorticity, $\Gamma(s, \theta)$, the Poisson-like Eq. (17), rewritten as

$$\frac{\partial}{\partial s} \left\{ \frac{R}{H} \frac{\partial \psi}{\partial s} - \omega R^2 \right\} + \frac{1}{R} \frac{\partial}{\partial \theta} \left\{ \frac{1}{H} \frac{\partial \psi}{\partial \theta} \right\} = RH\Gamma \quad (20)$$

must be solved to obtain the stream function, $\psi(s, \theta)$. From this solution new values for $\psi(s, \theta)$, $u_s(s, \theta)$ and $u_\theta(s, \theta)$ can then be calculated. Appropriate boundary conditions on ψ for use in the solution of Eq. (20) are:

(i) Along $s=0$, we specify an inlet swirl velocity, $u_\theta(0, \theta)$, which, in order to satisfy conservation of angular momentum, should normally be put equal to the swirl velocity in the reservoir upstream of the inlet.

(ii) An appropriate boundary condition at discharge, $s=S$, would be that the pressure in the flow exiting the annulus should be uniform for all θ ,

$$\frac{\partial}{\partial \theta} (p + \zeta u_s^2)_{s=S} = 0 \quad (21)$$

for a given exit loss coefficient, ζ . This parameter, ζ , can also be used to simulate an exit seal.

(iii) The periodic conditions on boundaries at $\theta=0$ and $\theta=2\pi$ such that

$$\psi(s, 2\pi) - \psi(s, 0) = Q \quad (22)$$

(2) Second, given the new values of $\psi(s, \theta)$, $u_s(s, \theta)$ and $u_\theta(s, \theta)$, we can integrate to find new values for $\Gamma(s, \theta)$ using Eq. (18). This requires evaluation of the shear stress functions, g_R and g_S and values of Γ at inlet, $\Gamma(0, \theta)$. Clearly this becomes more cumbersome when there is reverse flow either at inlet or at discharge. Here, we restrict our attention to the simpler circum-

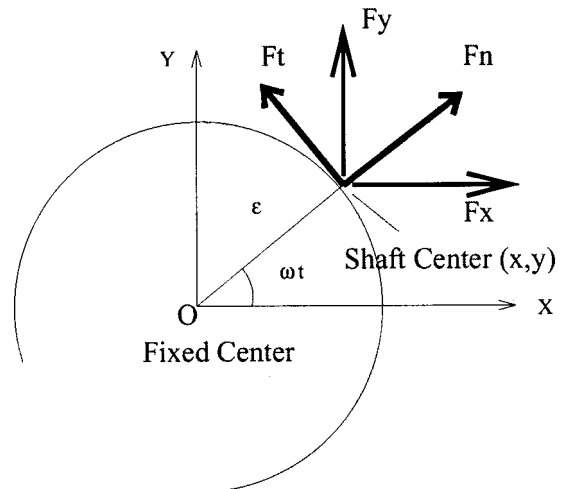


Fig. 2 Force diagram in plane normal to the shaft axis

stances in which there is no flow reversal at the inlet. Then, assuming that the viscous stresses upstream of the inlet are negligible and that the inlet flow is circumferentially uniform, Eq. (14) provides an initial value for Γ ,

$$\Gamma(0, \theta) = \frac{1}{Hu_s} [(u_\theta + \omega R)(g_s + g_R) + \Omega R g_R] \quad (23)$$

given the results from step 1.

These two steps are then repeated to convergence.

As the viscous terms were found to be small, Eq. (19) can be integrated in parallel to the Γ integration to obtain the total pressure throughout the domain. If entrance losses are neglected between the upstream reservoir and the inlet plane ($s=0$), then the integration begins with a uniform value of $P(0, \theta)$ equal to the total pressure in the reservoir, P_{res} , and this can conveniently be chosen to be zero without loss of generality. On the other hand if entrance losses are to be included then $P(0, \theta)$ can be set to a value smaller than P_{res} by an amount equal to the entrance loss at that particular θ position. Other complications which could be incorporated include a non-uniform upstream reservoir (such as the volute of a pump operating off-design) which would imply a circumferentially varying $P(0, \theta)$.

Having obtained the pressure (and the viscous shear stresses), it only remains to integrate these to obtain the normal and tangential forces acting on the rotor. With the sign convention as defined in Fig. 2, it follows that:

$$F_n = \int_0^S \left\{ 1 - \left(\frac{dR}{ds} \right)^2 \right\}^{1/2} \int_0^{2\pi} (p \cos \theta + \tau_{R\theta} \sin \theta) R d\theta ds \quad (24)$$

$$F_t = \int_0^S \left\{ 1 - \left(\frac{dR}{ds} \right)^2 \right\}^{1/2} \int_0^{2\pi} (p \sin \theta - \tau_{R\theta} \cos \theta) R d\theta ds \quad (25)$$

In the results quoted in this paper the contributions from the τ_{R0} parts of these integrals are very small and can often be neglected. Finally, the rotordynamic coefficients are obtained by fitting quadratics to the functions, $F_n(\omega/\Omega)$ and $F_t(\omega/\Omega)$,

$$F_n = M \left(\frac{\omega}{\Omega} \right)^2 - c \left(\frac{\omega}{\Omega} \right) - K \quad (26)$$

$$F_t = -C \left(\frac{\omega}{\Omega} \right) + k \quad (27)$$

The coefficients are termed the direct added mass (M), direct damping (C), cross-coupled damping (c), direct stiffness (K), and cross-coupled stiffness (k). The forces and coefficients are nondimensionalized as described by Brennen [1].

Results

The computational model was tested on two sets of geometries for which reliable experimental data is available. One comparison was with the seal tests conducted by Marquette and Childs [19]. This seal had an axially uniform radius, with a length to radius ratio of 0.914 and an average clearance of 0.0029 of the radius. Rotor speed varied from 10400 rpm to 41600 rpm and pressure drops from 4 MPa to 12 MPa. The other comparison is with the conical dummy pump impeller tested by Uy [20] whose eye-to-tip ratio is 0.474 and its average leakage path clearance is 0.03 times the tip radius. One difference between the two flows is the presence of the exit seal for the impeller tests. About half of the total pressure drop in the leakage path for the conical impeller occurs in the exit seal. Another difference is that the clearance is about an order of magnitude smaller for the seal experiments than for the impeller experiments. This will affect the acceleration of u_θ .

Using the same parameter values as Marquette and Childs, $n_s = n_r = 0.079$ and complete exit loss ($\zeta=0$), the rotordynamic force for the seal in the tangential direction is predicted very well by the current model as shown in Fig. 3. The normal force, however, exhibits a large but uniform offset from the experimental data as manifested by the discrepancy in K . The predictions are similar to those using the Childs' perturbation approach, suggesting dominance of the primary mode in this simple geometry.

Adjusting the exit loss coefficient, ζ , can mostly eliminate the discrepancy in the normal forces. Indeed the forces seem very sensitive to small changes in the exit condition. Whether the source of the large offset between theory and experiment can be appropriately attributed to the exit conditions remains unknown.

An examination of the accuracy of the calculated results from the bulk flow model was also carried out by comparing the rotordynamic forces for the conical impeller to the experimental data. As a result of direct measurements of inlet swirl [21], an inlet swirl velocity of $u_\theta(0, \theta) = 0.26$ was used for calculations of rotordynamic forces with the conical pump impeller geometry. Nu-

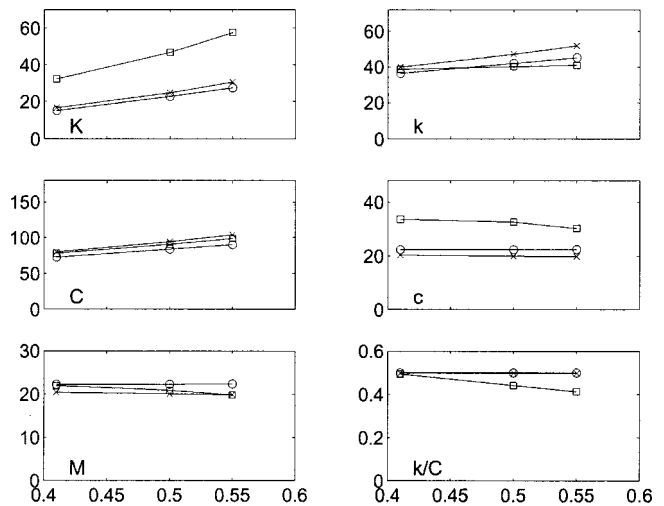


Fig. 3 Comparison of rotordynamic coefficients versus flow coefficient ϕ between experiment (\square), and current model (\circ), and Childs' perturbation model (\times) for the seal, with eccentricity equaling 10 percent of average clearance

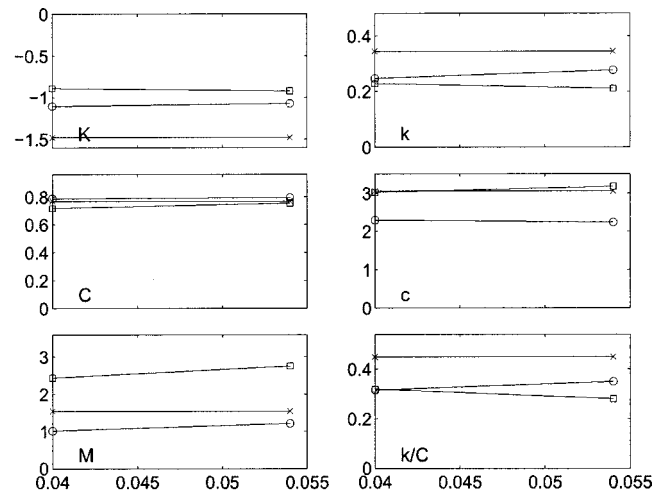


Fig. 4 Comparison of rotordynamic coefficients versus flow coefficient ϕ between experiment (\square), and current model (\circ), and Childs' perturbation model (\times) for the conical impeller

merical results for flow coefficients of 0.04 and 0.053 are compared with experimental measurements in Fig. 4. This data uses $n_s = n_r = 0.079$ for the shear stress coefficients and no pressure recovery at exit ($\zeta = 0$). The tangential forces agree reasonably well with the experimental data. The calculated normal forces, however, exhibit added mass, M , and cross-coupled damping, c , coefficients that are much smaller than the experimental results. The direct stiffness, K , agrees well with the experiments.¹

Figure 4 also shows the calculated rotordynamic coefficients using Childs' perturbation model. Compared with the Childs' model, the current model gives better predictions for the direct stiffness and cross-coupled stiffness coefficients as well as the whirl ratio, k/C . The direct damping coefficient, C , is well predicted by both, while both underpredict the added mass term significantly. Childs' model gives more accurate results for the cross-coupled damping coefficient. Calculations of the rotordynamic coefficients for two other contoured dummy impellers tested by Uy [20] yielded similar comparisons.

Conclusions

This paper has explored some of the basic characteristics of the bulkflow model equations for the turbulent flow in a fluid-filled annulus generated by a combination of rotational and whirling motions. The analysis unveils the definition of the appropriate vorticity for these flows and develops evolutionary equations both for the vorticity and for the total pressure, without resorting to linearization. Among other features demonstrated by these equations is the fact that the changes in vorticity and total pressure along a streamline are entirely due to the shear stresses imposed on the flow.

This equation structure naturally suggests a way in which numerical solutions to these equations might be sought, by iterating between a Poisson-like equation for the streamfunction using a preliminary vorticity distribution and forward integration to revise that distribution. Several sample calculations are used to illustrate this technique.

The numerical solutions are compared to experimental results for a seal geometry in addition to discharge-to-inlet leakage geometries. Results for the seal show very good agreement for the tangential forces. Predictions for the normal forces, however, exhibited a large offset to the experimental results, which can be reduced by changing the exit loss coefficient. Questions remain as to the reason for this discrepancy.

For leakage path geometries, good agreement with experimental results for the conical impeller was found with the exception of the added mass term. Compared to the Childs' perturbation solution method, the current method is more computationally intensive, though still relatively fast. It also provided better predictions for most of the rotordynamic coefficients with the exception of cross-coupled damping term.

Nomenclature

- C = direct damping coefficient, normalized by $\rho \pi \Omega^2 R_2^2 L \varepsilon$
 c = cross-coupled damping coefficient, normalized by $\rho \pi \Omega^2 R_2^2 L \varepsilon$
 F_n = force normal to whirl orbit, normalized by $\rho \pi \Omega^2 R_2^2 L \varepsilon$
 F_t = force tangent to whirl orbit, normalized by $\rho \pi \Omega^2 R_2^2 L \varepsilon$
 H = clearance between impeller shroud and housing

- K = direct stiffness coefficient, normalized by $\rho \pi \Omega^2 R_2^2 L \varepsilon$
 k = cross-coupled stiffness coefficient, normalized by $\rho \pi \Omega^2 R_2^2 L \varepsilon$
 L = axial length of the impeller
 M = direct added mass coefficient, normalized by $\rho \pi R_2^2 L \varepsilon$
 m_r, m_s = empirical exponent for rotor and stator respectively
 n_r, n_s = empirical constants for rotor and stator respectively
 P = total pressure
 p = static pressure
 Q = volumetric leakage flow rate
 R = radius of rotor
 R_2 = tip radius of the rotor
 u_s = meridional velocity of fluid
 u_θ = circumferential velocity of fluid, nondimensionalized by ΩR_2
 Γ = effective vorticity defined by Eq. (17)
 η = fluid viscosity
 ε = eccentricity of whirl orbit
 ζ = exit loss coefficient
 ρ = fluid density
 ϕ = leakage flow coefficient, $Q/2\pi H \Omega R_2^2$
 ψ = stream function, defined by Eq. (10)
 ω = whirl radian frequency
 Ω = main shaft radian frequency
 τ = wall shear stress

References

- [1] Brennen, C. E., 1994, *Hydrodynamics of Pumps*, Concepts ETI and Oxford University Press.
- [2] Childs, D. W., and Dressman, J. B., 1982, "Testing of Turbulent Seals for Rotordynamic Coefficients," *Proc. Workshop on Rotordynamic Instability Problems in High-Performance Turbomachinery*, NASA Conf. Publ. 2250, 157-171.
- [3] Nordmann, R., and Massmann, H., 1984, "Identification of Dynamic Coefficients of Annular Turbulent Seals," *Proc. Workshop on Rotordynamic Instability Problems in High Performance Turbomachinery*, NASA Conf. Publ. 2338, 295-311.
- [4] Guinzburg, A., Brennen, C. E., Acosta, A. J., and Caughey, T. K., 1994, "Experimental Results for the Rotordynamic Characteristics of Leakage Flows in Centrifugal Pumps," *ASME J. Fluids Eng.*, **116**, pp. 110-115.
- [5] Childs, D. W., 1987, "Fluid Structure Interaction Forces at Pump-Impeller-Shroud Surfaces for Rotordynamic Calculations," *ASME Symp. on Rotating Machinery Dynamics*, **2**, 581-593.
- [6] Childs, D. W., 1989, "Fluid Structure Interaction Forces at Pump-Impeller-Shroud Surfaces for Rotordynamic Calculations," *ASME J. Vib. Acoust. Stress, Reliab. Des.*, **111**, pp. 216-225.
- [7] Guinzburg, A., 1992, *Rotordynamic Forces Generated by Discharge-to-Suction Leakage Flows in Centrifugal Pumps*, Ph.D. thesis, Calif. Inst. of Tech, Pasadena, CA.
- [8] Hirs, G. G., 1973, "A Bulk-Flow Theory for Turbulence in Lubricant Films," *ASME J. Lubr. Technol.*, Apr. pp. 137-146.
- [9] Sivo, J., Acosta, A. J., Brennen, C. E., Caughey, T. K., Ferguson, T., and Lee, G., 1994, "Laser Velocimeter Measurements in the Leakage Annulus of a Whirling Centrifugal Pump," *ASME Laser Anemometry-1994, Advances and Applications*, FED-191, 111-117.
- [10] Guelich, J., Florjancic, D., and Pace, S., 1989, "Influence of Flow Between Impeller and Casing on Part-Load Performance of Centrifugal Pumps, Pumping Machinery," 3rd Joint ASCE/ASME Mechanics Conference, **81**, 227-235.
- [11] Baskharone, E., and Hensel, S., 1993, "Flow Field in the Secondary, Seal-Containing Passages of Centrifugal Pumps," *ASME J. Fluids Eng.*, **115**, pp. 702-709.
- [12] Black, H. F., 1969, "Effects of Hydraulic Forces in Annular Pressure Seals on the Vibrations of Centrifugal Pump Rotors," *J. Mech. Eng. Sci.*, **11**, No. 2, pp. 206-213.
- [13] Black, H. F., and Jensen, D. N., 1970, "Dynamic Hybrid Properties of Annular Pressure Seals," *Proc. J. Mech. Eng.*, **184**, pp. 92-100.
- [14] Childs, D. W., 1983, "Dynamic Analysis of Turbulent Annular Seals Based on Hirs' Lubrication Equation," *ASME J. Lubr. Technol.*, **105**, pp. 429-436.
- [15] Childs, D. W., 1983, "Finite Length Solutions for Rotordynamic Coefficients of Turbulent Annular Seals," *ASME J. Lubr. Technol.*, **105**, pp. 437-445.
- [16] Childs, D. W., and Scharrer, J. K., 1986, "Experimental Rotordynamic, Coef-

¹The highest inlet swirl ratio presented was 0.27, because this is the highest experimental data available [21]. At higher inlet swirl ratios, resonances occur in Childs' perturbation calculations. The current method also exhibits some resonance behavior, but the rotordynamic force curves always remain smooth. Further details can be found in [21].

ficient Results for Teeth-on-Rotor and Teeth-on-Stator Labyrinth Gas Seals," *Proc. Adv. Earth-to-Orbit Propulsion Tech. Conf., NASA Conf. Publ. 2436*, 327–345.

- [17] Pinkus, O., and Sternlicht, B., 1961, *Theory of Hydrodynamic Lubrication*, McGraw-Hill, New York.
- [18] Fritz, R. J., 1970, "The Affects of an Annular Fluid on the Vibrations of a Long Rotor," *ASME J. Basic Eng.*, **92**, pp. 923–937.
- [19] Marquette, O. R., Childs, D. W., SanAndres, L., 1997, "Eccentricity Effects on

the Rotordynamic Coefficients of Plain Annular Seals: Theory Versus Experiment," *ASME J. Tribol.*, **119**, pp. 443–447.

- [20] Uy, R. V., and Brennen, C. E., 1999, "Experimental Measurements of Rotordynamic Forces Caused by Front Shroud Pump Leakage," *ASME J. Fluids Eng.*, **121**, pp. 633–637.
- [21] Hsu, Y., 2001, *Studies of Rotordynamic Forces Generated by Discharge-to-Suction Leakage Flows in Centrifugal Pumps*, Ph.D. thesis, Calif. Inst. of Tech, Pasadena, CA.